JOURNAL OF MATERIALS SCIENCE 27 (1992) 2298–2308

Microstructures of explosively consolidated rapidly solidified aluminium and Al–Li alloy powders

JIN-YUAN ZHANG, BAOREN AI, CHUNLAN LIU, RUIZHEN ZHU
Central Iron and Steel Research Institute, 100081 Beijing, People's Republic of China
DENGXIA ZHANG, CHENGHUI MA
Institute of Mechanics, Academina Sinica, 100080 Beijing, People's Republic of China

The microstructures and the characteristics of water-atomized, nitrogen gas-atomized Al powders and ultrasonic argon gas-atomized Al–Li alloy powder were investigated by means of metallography, SEM, Auger electron spectroscopy and X-ray diffraction techniques. Rapidly solidified powders were explosively consolidated into different sized cylinders under various explosive parameters. The explosively consolidated compacts have been tested and analysed for density microhardness, retention of rapidly solidified microstructures, interparticle bonding, fractography and lattice distortion. It is shown that the explosive consolidation technique is an effective method for compacting rapidly solidified powders. The characteristics of surface layers play a very important role in determining the effectiveness of the joints sintered, and the Al–Li alloy explosive compacts present an abnormal softening appearance compared to the original powder.

1. Introduction

It is now documented that a rapidly solidified (RS) powder possesses a series of advantages, such as fine grain size, removal of macro-segregation and reduction in scale of micro-segregation, supersaturated solid solutions and metastable phases retained. These characteristics in microstructure may make the properties of materials and products made from RS powders very attractive. The key to the equation is that the inherent benefits of rapid solidification are not lost during the process of powder consolidation.

On the other hand, it is almost impossible to prevent the formation of a tenacious oxide film on aluminium, since a partial pressure of oxygen of less than 10^{-53} atm would be required for an oxide-free surface [1]. In general, there always exists an oxide film on the surface of aluminium or aluminium alloy; moreover, its thickness, composition and uniformity may depend on the composition of the alloy, the powder particle size, the time and conditions of storing the powder and the process by which it was prepared. An adsorbed film such as H_2O/O_2 can be removed by degassing the powder at about 200 °C, but an Al_2O_3 film on powder particles cannot be reduced by any reducing agent. It is perhaps the reason why aluminium powder cannot be easily sintered.

In view of the facts mentioned above, it is necessary to exploit a special technique for consolidating rapidly solidified powder into a bulk microcrystalline material. This consolidating process should be capable of retaining the inherent benefits of RS powder, of fragmenting and dispersing the unavoidable oxide film on the powder particle surfaces, and of providing a suitable compact for subsequent treatments so as to improve the properties further.

According to published reports [2–5] and our experience, explosive consolidation is an effective process for compacting RS powder in which powder densification is achieved by a high-pressure shock wave. The shock waves can be created in materials by the detonation of an explosive in contact with the material or by the impact of a projectile on the material. During the passage of the shock wave, a high loading rate occurs. The associated pressures greatly exceed the shear strength of the alloy to be compacted so that the powder particles are plastically deformed, which causes the oxide film to disintegrate and reduces the gaps between powder particles. There is also a lot of relative movement of the particles over one another while the shock wave passes, so that friction leads the local temperature to transiently rise. It is possible that individual particles collide under such conditions that surface melting, explosive welding and jointing are likely to occur. The heat is not generated uniformly over the whole volume of the compact during explosive consolidation. It is more or less limited to the surface of the individual particles. The excellent environment resulting from the explosive process is that most parts of the compact remain at a relatively low temperature while more rapid heating and cooling on the particle surfaces occur. It is easy to understand that grain-coarsening and precipitation

0022–2461

TABLE I Particle size distribution of Al and Al–Li powders used in explosive consolidation experiments

Size range (μm)	Distribution (wt %)		
	Water-atomized Al powder	N_2-atomized Al powder	Ar-atomized Al–Li powder
< 10	3.6	4.6	0.9
10–20	15.0	13.2	2.3
20–30	23.1	17.9	9.0
30–40	20.6	14.2	12.7
40–50	18.2	14.0	6.9
50–60	18.0	9.0	11.3
60–70	0.7	11.0	17.8
70–80	0.6	6.6	7.3
80–90	0	4.2	16.8
90–100	0	5.3	14.9
Median size (μm)	34	40	64
Specific surface ($m^2 g^{-1}$)	0.127	0.081	0.048

TABLE II Apparent density and tap density of Al and Al–Li powders

	Water-atomized Al powder	N_2-atomized Al powder	Ar-atomized Al–Li powder
Apparent density ($g cm^{-3}$)	1.08	1.20	1.38
Tap density ($g cm^{-3}$)	1.49	1.71	1.71

are not only essentially avoided but also a region with ultra-fine crystallites appears at the particle interfaces during the explosive consolidation process.

A series of experiments on explosive consolidations of water-atomized, nitrogen gas-atomized Al powders and ultrasonic argon gas-atomized Al–Li powder have been made. In this paper, the microstructures of different starting powders and various powder compacts are described. Based on these analyses, we attempted to address the factors which are of great importance to the performance of explosive compaction.

2. Characteristics of rapidly solidified powders

The Al powders were prepared by water atomization or nitrogen gas atomization and Al–1.40Li–4.60Cu–0.54Mg–0.16Zr (designated as Al–Li) alloy powder prepared by the ultrasonic argon gas atomization technique. The powders were stored in different ways (water-atomized Al in air, nitrogen-atomized Al in a vacuum, argon-atomized Al–Li alloy under dry argon) from the time they were prepared until they were used for consolidation.

Powder particle size distributions were determined using a centrifugal photo-sedimentor model SA-CP3 and the results are listed in Table I. Apparent densities and tap densities of various powders were measured using standard apparatus and the results are listed in Table II.

Scanning electron micrographs of the powders are shown in Figs 1 to 3. It can be seen from the micrographs that the morphology of ultrasonic argon-atomized Al–Li alloy powder (Fig. 3) is largely spherical with a significant number of satellites; that of nitrogen-atomized powder (Fig. 2) is spherical for smaller particles and ellipsoidal for bigger ones; and that of water-atomized powder (Fig. 1) is relatively irregular, being angular, ellipsoidal, branched, etc.

The atomization process can be considered as an extremely small casting of the order of 1 μg. This mass is allowed to cool rapidly from a molten state at a rate which is many orders of magnitude greater than that employed in conventional casting. The cooling rates for solidifications of different sized droplets can be calculated from the atomizing parameters concerned [6] or estimated from the microstructures of powder particles. For aluminium alloy, the average dendrite arm spacing, λ (μm) may be related to the cooling rate, ε ($K s^{-1}$) by the equation [7]

$$\lambda = 50\varepsilon^{-1/3}$$

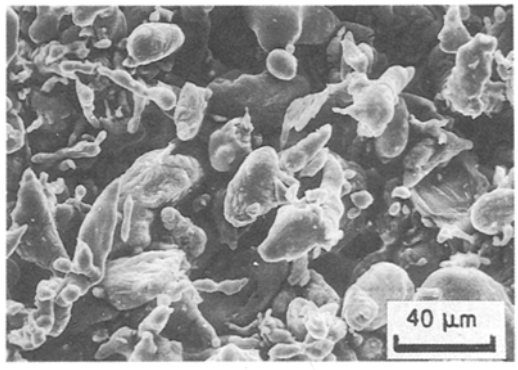

Figure 1 Scanning electron micrograph of water-atomized Al powder.

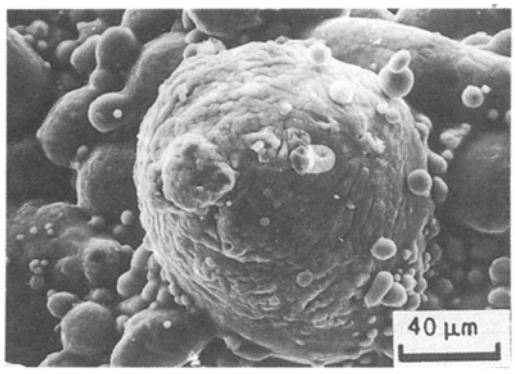

Figure 2 Scanning electron micrograph of N_2-atomized Al powder.

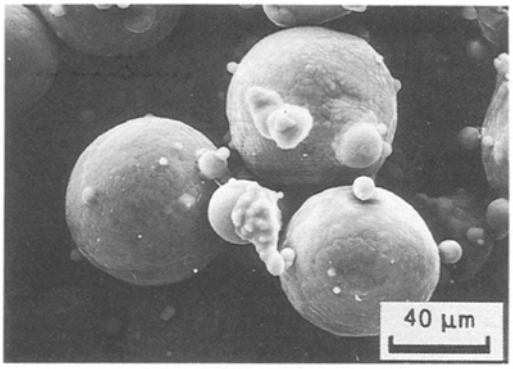

Figure 3 Scanning electron micrograph of ultrasonic argon-atomized Al–Li alloy powder.

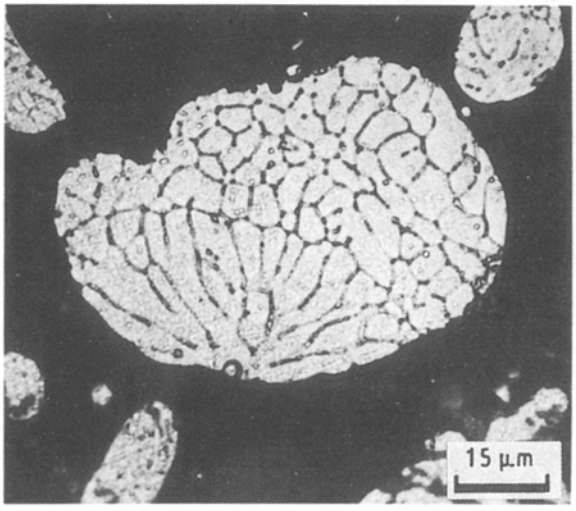

Figure 4 Microstructure of water-atomized Al powder.

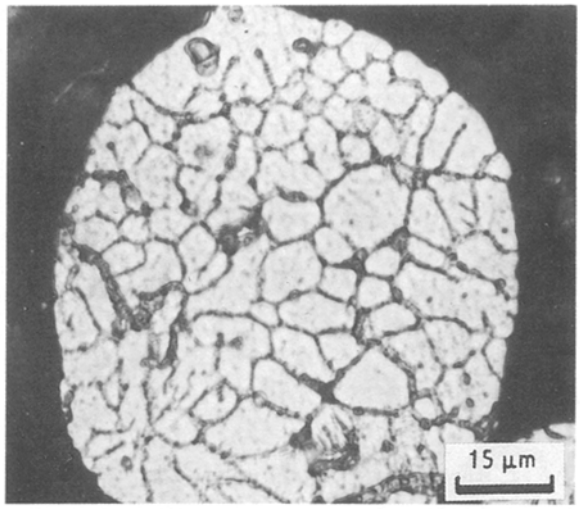

Figure 5 Microstructure of N_2-atomized Al powder.

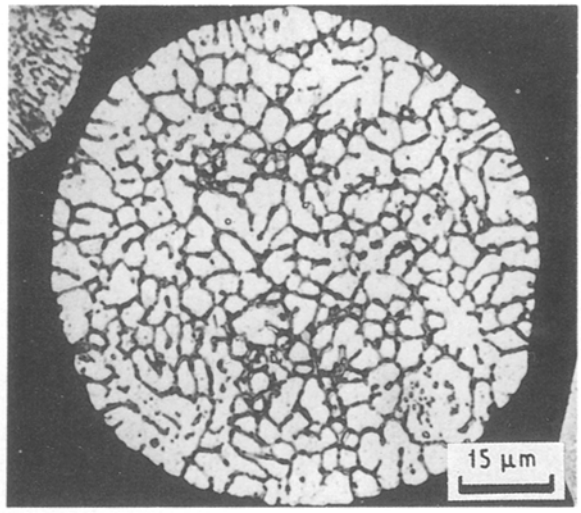

Figure 6 Microstructure of ultrasonic argon-atomized Al–Li powder.

Figs 4, 5 and 6 show the microstructures corresponding to water-atomized, nitrogen-atomized and ultrasonic argon-atomized powder, respectively. As can be seen, the powders generally consist of mixed equiaxed-dendritic types of structure. The average values were measured to be 4.2 μm (Fig. 4, water-atomized 50 μm particle), 6.2 μm (Fig. 5, nitrogen-atomized 70 μm particle), and 3.2 μm (Fig. 6, ultrasonic argon-atomized 80 μm particle), so that the cooling rates deduced from the equation are about 1.7×10^3, 5.2×10^2 and 3.8×10^3 K s^{-1}, respectively. The smaller the powder particles, the greater the cooling rate experienced by them. In general, it may be expected that the cooling rates as different powder particles form are 10^2–10^5 K s^{-1}, since most particles are smaller than those illustrated in the figures above.

The Vickers microhardness was measured using a microhardness tester model MT-3 on powder embedded in resin and polished. The results are 23.7 ± 1, 22.7 ± 0.4 and 86.4 ± 3.9 kg mm^{-2} for water-atomized Al, nitrogen-atomized Al and argon-atomized Al–Li alloy powder, respectively. The hardness of Al–Li alloy powder is much higher than those of Al powders, which indicates alloying hardening.

As mentioned above, the state of the oxide film on the surfaces of Al and Al alloy powders plays an important role in their consolidation. The contents of oxygen in the three kinds of powder were determined using a infrared absorption spectrometer model TC-136. The results are shown in Table III.

In order to investigate the thickness and composition of oxide films on different kinds of powder particle, they were pressed on to indium foils and then the

TABLE III Oxygen content (wt %) of Al and Al–Li powders

Water-atomized Al powder	N_2-atomized Al powder	Ar-atomized Al–Li powder
0.23	0.085	0.025

surfaces of the powders were analysed using a scanning Auger spectrometer model PHI-595. Compositional depth profiles were obtained by recording the relative intensities of O and Al peaks while sputtering with Ar ions at a material removal rate of approximately 10 nm min^{-1}.

The Auger electron spectra of the uppermost surfaces for different powders with a particle size of about 50 μm are shown in Fig. 7. Fig. 8 shows the spectra of the surfaces after sputtering for one minute. Fig. 9 displays the compositional depth profiles of O and Al for the three kinds of powder. It can be seen that the water-atomized powder has a thicker oxide layer which is about 50–60 nm thick; the thickness of oxide film for nitrogen-atomized powder is about 20–30 nm, and only about 5 nm for ultrasonic argon-atomized powder. It was noticed from the spectra that there are some contaminants such as C, Si etc. on the surfaces of the powder but Cu could not be detected on the uppermost surface of Al–Li alloy powder. The compositional depth profile was also determined for Al–Li alloy powder with a larger particle size (~ 200 μm) by recording the relative intensities of O,

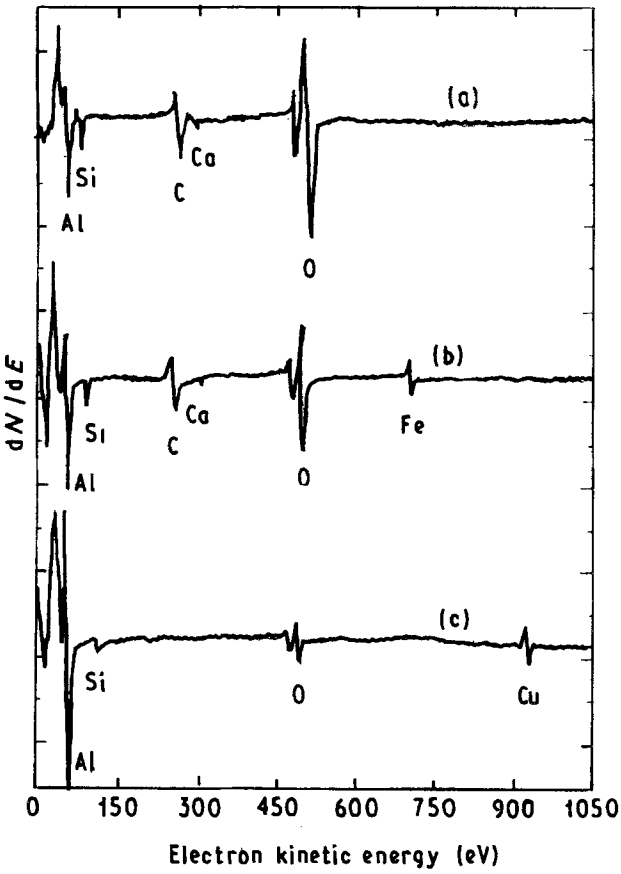

Figure 8 Auger electron spectra recorded from powder particles after ion sputtering for 1 min: (a) water-atomized Al powder, (b) N_2-atomized Al powder, (c) ultrasonic argon-atomized Al–Li alloy powder.

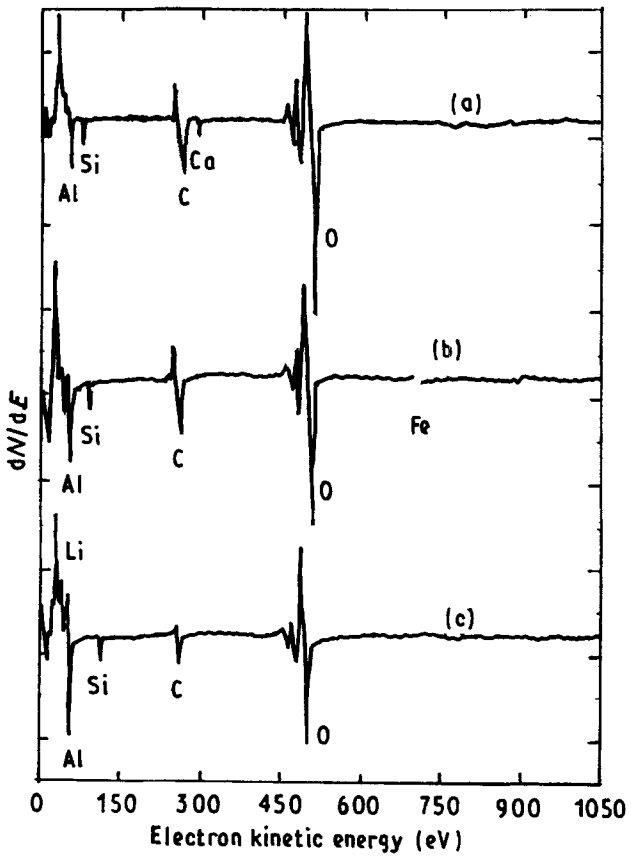

Figure 7 Auger electron spectra recorded from powder particles before ion sputtering: (a) water-atomized Al powder, (b) N_2-atomized Al powder, (c) ultrasonic argon-atomized Al–Li alloy powder.

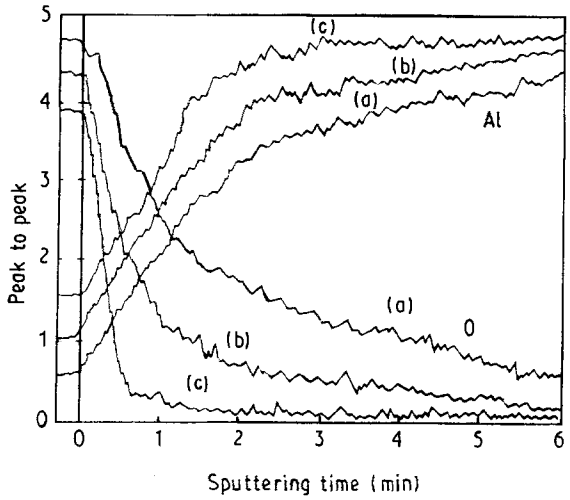

Figure 9 Results of AES analyses of powder particles given as peak-to-peak intensity of Al and O versus sputtering time: (a) water-atomized Al powder, (b) N_2-atomized Al powder, (c) ultrasonic argon-atomized Al–Li alloy powder.

Al, Li and Mg signals. The results are shown in Fig. 10, from which it can be seen that there exists an Li- and Mg-rich oxide film with a thickness of about 10 nm on the surface of Al–Li alloy powder. Referring to the report of Gilman and Sankaran [8], the oxide layer on the surface of this alloy powder and its redistributions during consolidation may be expected to be as shown in Fig. 11.

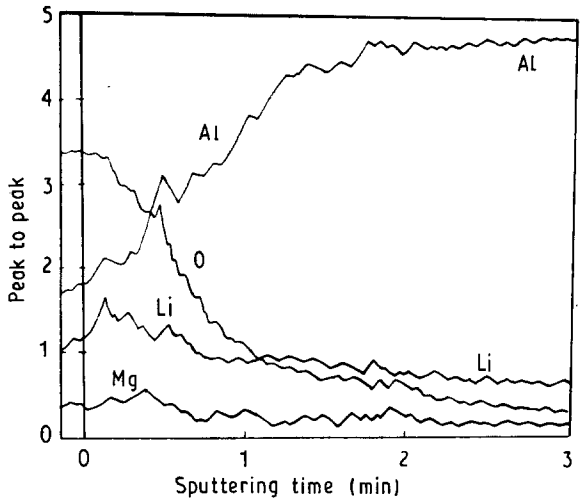

Figure 10 Depth profile of Al, O, Li and Mg recorded from one Al–Li alloy powder particle with a size of about 200 μm.

X-ray diffraction experiments on the RS powders were carried out for phase analyses, lattice parameter determinations and diffraction profile analyses. It was discovered that $Al(OH)_3$ and SiO_2 are present in all of the powders. The former may be considered as a hydroxide film, the latter as a sort of contaminant. A metallic compound phase Al_7Cu_4Li was identified in the Al–Li alloy powder. Moreover, CoK_α radiation and the (3 1 1) diffraction line ($2\theta = 149°$) were chosen for determining the full width at half peak-height (FWHP) and the lattice parameter with a precision of $\pm 2 \times 10^{-5}$ nm. The lattice parameters of both Al powders are 0.40485 nm, which is very close to the parameter of pure Al, 0.40491 nm. The lattice parameter of ultrasonic argon gas-atomized Al–Li alloy powder was measured to be 0.40453 nm, which indicates that Cu and Li may partly dissolve in the matrix since the atomic radii of both elements are smaller than that of Al. The FWHPs of (3 1 1) diffraction lines for water-, nitrogen- and argon-atomized powders were measured to be 0.40, 0.39 and 0.47°, respectively, indicating that the lattice distortions are not serious.

3. Canning and explosive consolidation

Four kinds of capsule were used for the experiments. They are schematically illustrated in Fig. 12. They consist of single-tube type and double-tube type, as well as evacuated or unevacuated mode. Powders were poured into annealed mild steel cans of different sizes. In order to obtain a high tap density the powder packs were vibrated while filling. Some of them were evacuated at 150–200 °C for 1 h and then sealed. In general, the packing densities were 52–60% of the theoretical density for Al powders and 61–67% for the Al–Li alloy powder.

The experimental arrangements used for explosive consolidation are illustrated in Fig. 13a. The assembled powder pack is placed in the centre of the unburned explosive. The detonation is initiated at the upper end and a detonation wave proceeds in the axial direction. The extended explosive column above the powder pack ensures adequate development of a plane detonation wave which will travel longitudinally downward at the beginning of the powder compaction process. As the detonation wave propagates, the detonation pressure behind the wavefront compresses the powder pack or the fly-tube and consolidates the powder in the capsule. Fig. 13b shows the situation at some time after the initiation of detonation. The pressure exerted on the powder and its duration are functions of the composition and amount of explosive, the material and type of capsule, and the powder characteristics as well as the canning procedure. Even if the pressure behind the detonation wave in both single and double tube arrangements is the same, the magnitude of the peak pressure and the duration of the compacting pressure are different for the direct drive and the fly-tube drive cases.

Both the pressure and the duration determine the starting intensity of the shock wave exerted on the capsule wall. As it proceeds toward the centre of the cylindrical sample it meets powder in front of it and leaves compacted material behind it. There are two opposing effects. Due to the cylindrical arrangement the intensity of the shock wave increases toward the centre; however, as compaction of the powder occurs,

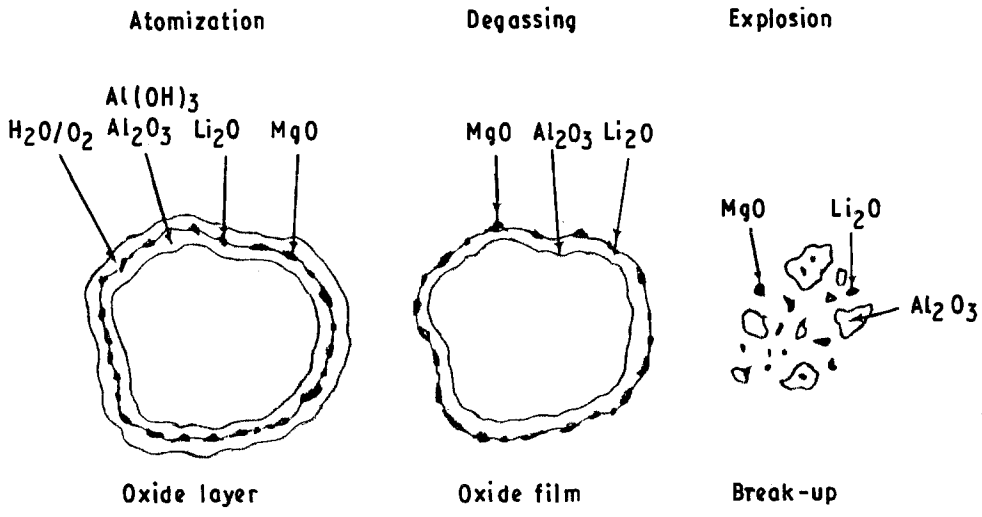

Figure 11 Removal and breakdown of oxide layer on Al–Li alloy powder particle during degassing and explosive consolidation.

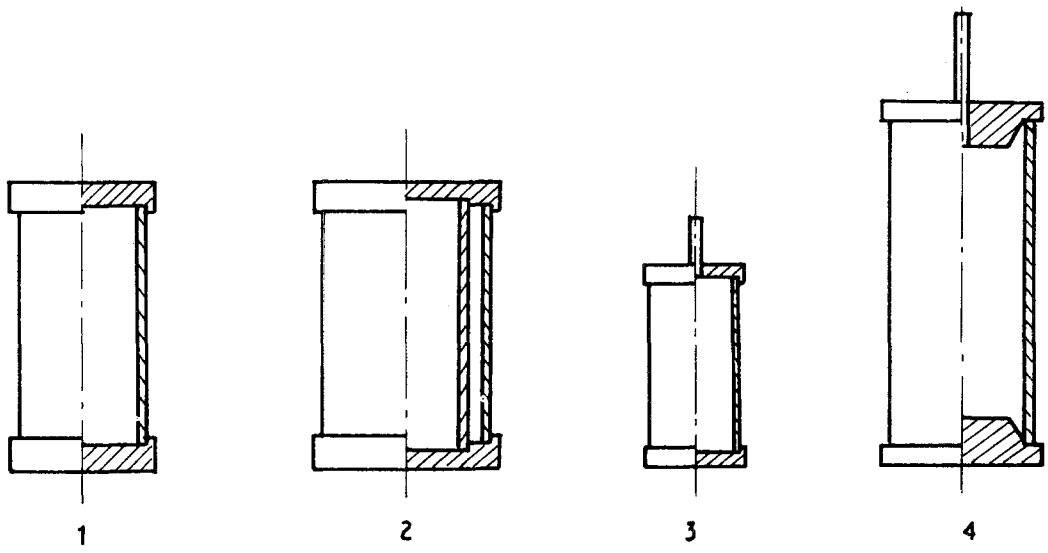

Figure 12 Schematic diagram of different types of capsule.

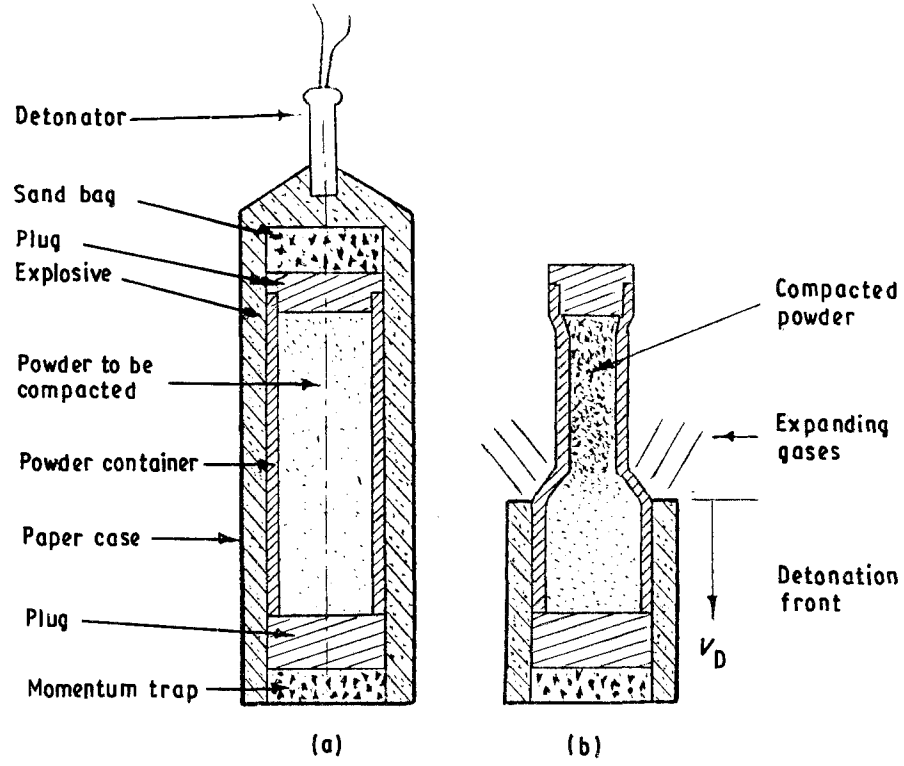

Figure 13 (a) Assembled powder pack ready for explosive consolidation. (b) A situation at some time after the initiation of detonation.

work is performed, leading to an attenuation of the shock wave. The two effects oppose each other and in the ideal case there is a balance between the two. If the absorption during compaction is too severe and a decreasing intensity of shock wave is the result of it, uncompacted material can be left in the centre. On the other hand, if the absorption is low the converging nature of the shock wave can give an overbalance, and a reflected wave at the centre leads to fracture of the already compacted sample. In severe cases, when the converging shock wave is forming a "Machstem" in the centre, molten material is thrown out leaving a hole in the centre of the compacted cylindrical sample.

On the basis of theoretical estimation, many parametric experiments on explosive consolidation were carried out and the optimizing conditions for consolidating RS Al and Al–Li alloy powders were found iteratively.

4. Experimental results and the microstructures of explosively consolidated compacts

Water-atomized Al powder was explosively consolidated into cylinders 70 mm in diameter and 110 mm long. Most of the specimens had circular cracks. Some had a "Mach-hole" in the centre. The samples for density testing (performed according to ISO 237B) were cut from different parts of each compact. The range of average density was measured to be

TABLE IV Microhardness and FWHP[a] of different powders and explosive compacts[b]

	W-A-P	N-A-P	UA-A-P	W-A-C	N-A-C	UA-A-C
H_v (kg mm^{-2})	23.7 ± 1.0	22.7 ± 0.4	86.4 ± 3.9	25.8 ± 1.0	25.7 ± 0.9	61.1 ± 4.9
FWHP (deg)	0.40	0.39	0.47	0.78	0.72	1.30

[a] FWHP: Full width at half peak height (CoK_α, (3 1 1) line).
[b] W-A-P: Water-atomized powder, N-A-P: N_2-atomized powder, UA-A-P: ultrasonic argon-atomized Al–Li alloy powder, W-A-C: compact from W-A-P, N-A-C: compact from N-A-P, UA-A-C: compact from UA-A-P.

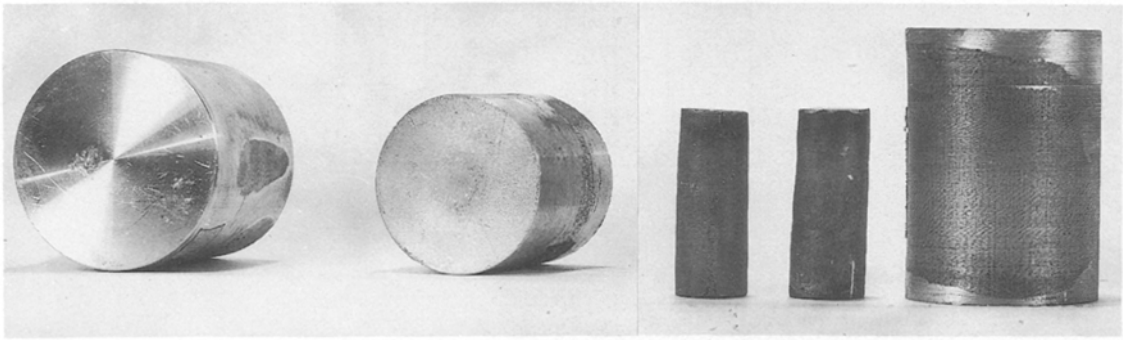

Figure 14 Typical photographs of explosive compacts prepared from Al and Al–Li alloy powders.

96.4–98.6% of the theoretical density for this kind of compact. For one compact, the density fluctuation measured was less than 5%. The maximum density at a local area in a compact could reach 99.6% of the theoretical density.

Nitrogen-atomized Al powder was explosively consolidated into 100 mm diameter, 110 mm long cylinders without any "Mach-hole" but some cracks. The range of the average relative density for this type of explosive compact was 97.9–99.2%.

Ultrasonic argon-atomized Al–Li alloy powder was explosively consolidated into 16 or 45 mm diameter, 60 mm long cylinders without any "Mach-hole" and crack. The range of the average relative density of this type of explosive compact was 97.0–99.1%.

Fig. 14 shows some typical photographs of compacts which were produced from Al and Al–Li alloy powders through explosive consolidation.

The microhardness was measured for different polished compacts. For comparison, the hardness values measured from the powders as well as from the compacts are given in Table IV. This shows that the two types of Al powder are slightly hardened but the Al–Li alloy powder is to a certain degree softened through explosive consolidation. The softened appearance of Al–Li alloy explosive compacts is contrary to the results given of Peng *et al.* [9] and difficult to interpret so far, but it is a real experimental phenomenon. It will be beneficial to the subsequent treatment of the explosive compact.

On the other hand, X-ray diffraction experiments on these explosive compacts display a significant broadening of profiles. The FWHPs of (3 1 1) diffraction lines obtained from different powders and compacts are also listed in Table IV. They indicate that lattice distortion occurs during explosive consolidation for all kinds of powder, especially for Al–Li alloy powder. The diffraction profiles in Fig. 15a and b were obtained from the Al–Li alloy powder and its compacts, respectively. It is clear that profile (b) is much broader than profile (a).

The explosively consolidated compacts were analysed by means of metallography and SEM in order to observe the retention of rapidly solidified microstructure, interparticle bonding and fractography. Fig. 16 shows micrographs and fractographs obtained from an explosive compact prepared from water-atomized Al powder. The relative density of the specimen analysed was as high as 99.4%. From Fig. 16a, it was concluded that the as-solidified microstructure in the original powder had been retained, but no real sintering between powder particles could be found in the compact. The particle boundaries can be seen clearly so that there are no effective joints between neighbouring particles. No melted zones or recrystallized regions were observed. Powder particles were compacted mainly by plastic deformation resulting from the action of the explosive shock wave. The joints obtained are fundamentally mechanical in nature (Fig. 16b). Fracture in this type of specimen is predominantly along the interparticle boundaries (Fig. 16d).

As mentioned above, the surfaces of the water-atomized powder particles are covered with a very thick (> 50 nm) oxide layer. This may be the main problem that influences the effective jointing between powder particles during explosive consolidation. In spite of the explosive shock wave being able to generate an intense plastic deformation at the periphery of the powder particles, however, it is insufficient to break up so thick an oxide layer. It is well known that an oxide such as Al_2O_3, with a high melting point (2015 °C) and low thermal conductivity, would behave as a thermal insulator, reducing heat transfer at particle surfaces and therefore possibly preventing surface melting. It is also easy to understand that without the breakdown of the surface oxide layers, contacts and

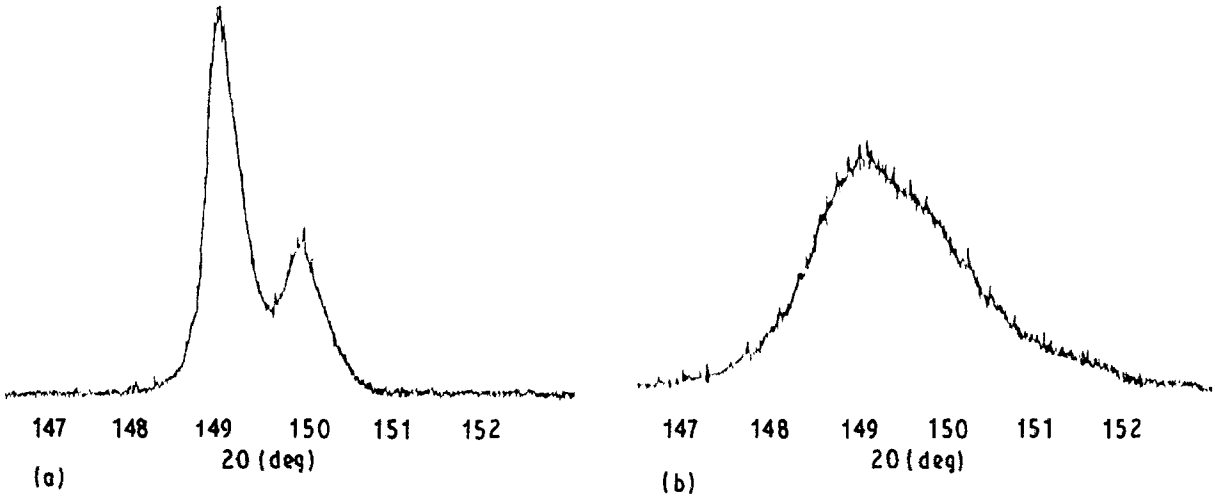

Figure 15 X-ray diffraction profile (a) obtained from Al–Li alloy powder, and (b) from its explosive compact.

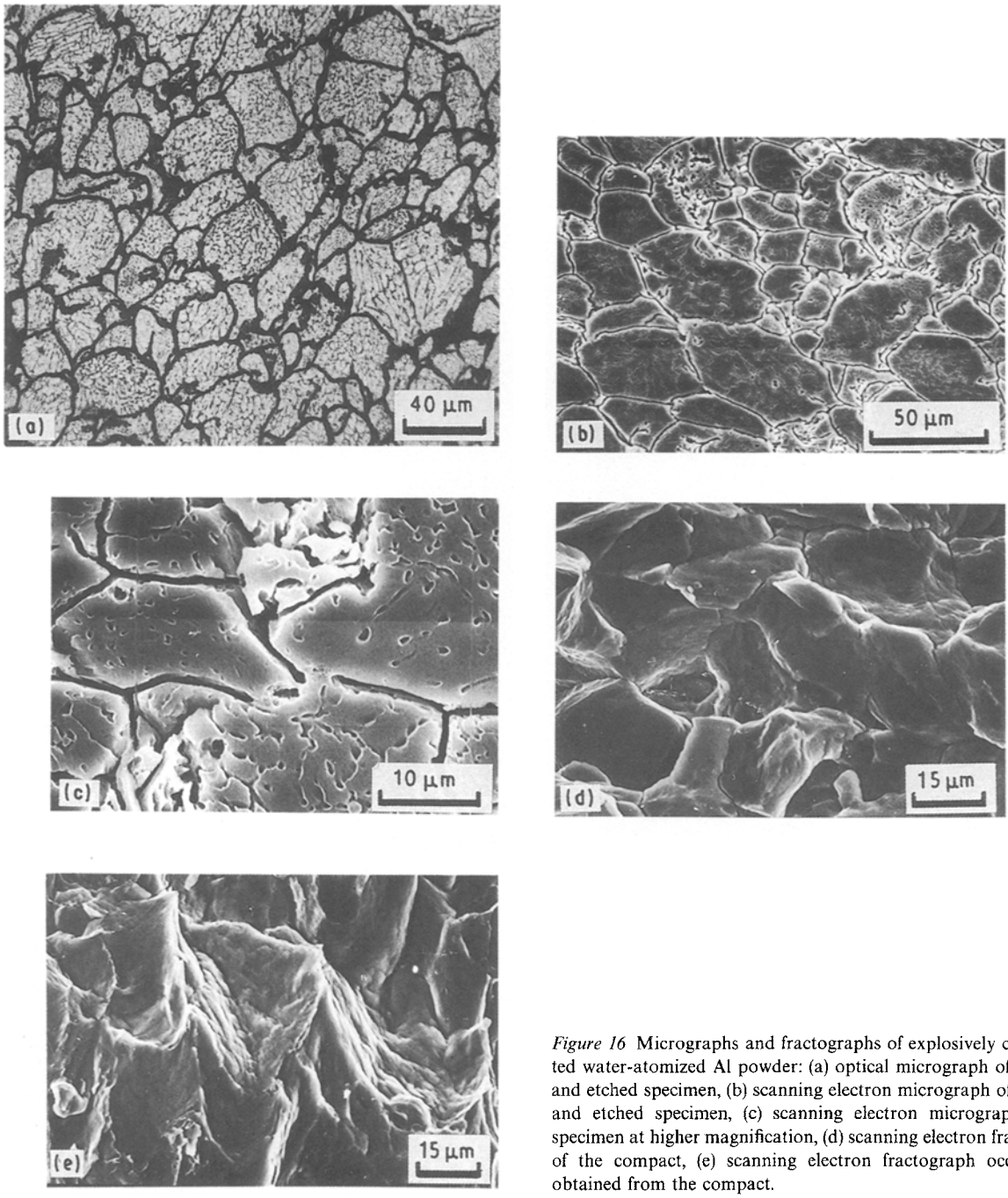

Figure 16 Micrographs and fractographs of explosively consolidated water-atomized Al powder: (a) optical micrograph of polished and etched specimen, (b) scanning electron micrograph of polished and etched specimen, (c) scanning electron micrograph of the specimen at higher magnification, (d) scanning electron fractograph of the compact, (e) scanning electron fractograph occasionally obtained from the compact.

joints of the fresh aluminium grains in the neighbouring particles cannot be expected, nor can acceptable mechanical properties of the explosive compact even though it may possess a high density.

It may be seen occasionally in an SEM micrograph at higher magnification (Fig. 16c) that welded bridges between neighbouring particles are established through breakdown of the surface oxide layers. Thus, a mixed mode of fracture was also observed consisting of brittle interparticle failure mixed with a transparticle ductile dimple fracture (Fig. 16e).

Typical micrographs and fractograph obtained from explosive compacts which were made from the N_2-atomized powder are shown in Fig. 17. It can be seen from Fig. 17a that the individual particles have lost their identity and the as-solidified dendritic structure is retained. A relatively effective joint between powder particles has been formed as a consequence of the breakdown of the surface oxide layers, which facilitates the formation of welded bridges and of a wavy interface. In the regions marked A (Fig. 17a and b), a cellular microstructure with very small cell diameter can be seen, which is evidently the result of melting and resolidification during explosive consolidation.

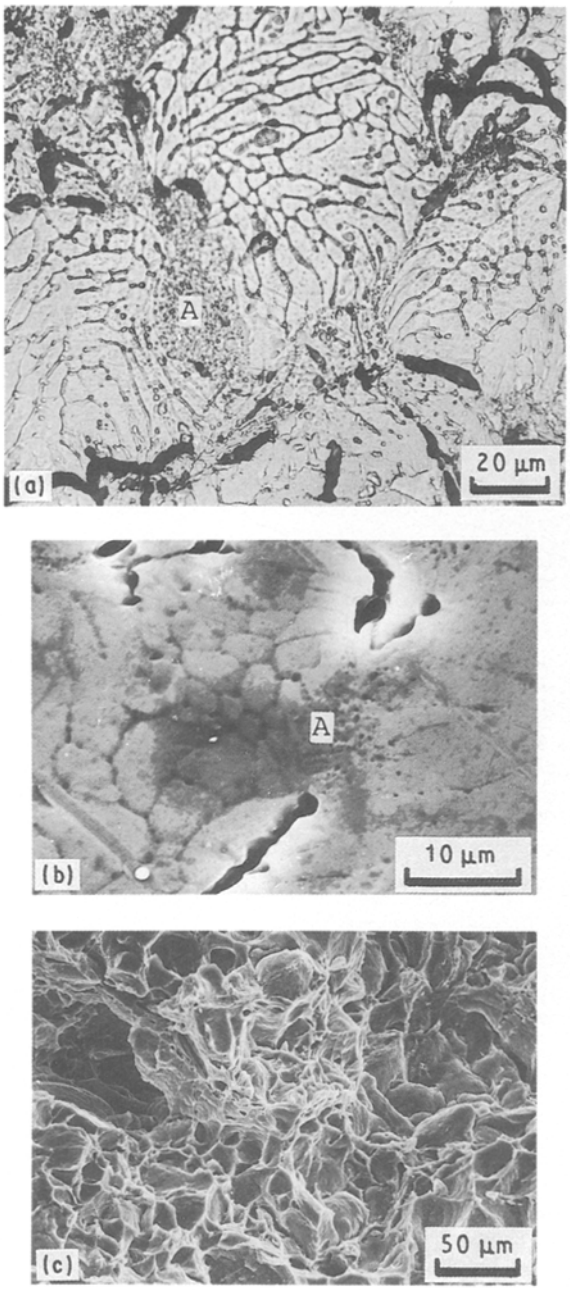

Figure 17 Micrographs and fractograph of explosively consolidated N_2-atomized Al powder: (a) optical micrograph of polished and etched specimen, (b) scanning electron micrograph of the specimen showing a resolidified zone, (c) scanning electron fractograph of the compact.

It has been known that the surface oxide layer of this powder is thinner than that of the water-atomized Al powder, which promotes the effectiveness of the joints between powder particles. It is likely from the micrograph that the breakdown of the surface oxide layers is still insufficient; therefore the bonding of the particles is due to various mechanisms, i.e. owing to both surface melting and mechanical compactness. The fractograph (Fig. 17c) of this specimen shows both fracture along the interparticle boundary and transparticle ductile dimple fracture.

Fig. 18 shows micrographs and fractographs obtained from explosive compacts prepared from the Ar-atomized Al–Li alloy powder. The oxide film on the surface of this type of powder particle is very thin and rich in Li and Mg, which will greatly facilitate their breakdown during explosive consolidation. It appears from Fig. 18a and b that powder particles are welded together through surface melting of themselves, and a sort of optically featureless region is formed surrounding the original powder particle interfaces. The SEM micrograph at higher magnification (Fig. 18c) shows that the featureless region marked A consists of cellular structure with a cell diameter of about 0.2 μm. It is evidently the result of melting and resolidification during explosive consolidation. The cooling rate of the liquefied portion of the powder particle surface was much higher compared with the conditions of atomization. The principal type of bonding of powder particles in this type of compact is metallurgical in nature, which is not able to be completed by the plastic deformation of powder particles above. Fractographs (Fig. 18d and e) show a very ductile dimpled interconnected fracture network surrounding the regions of interparticle failure. It was noted that there exist many precipitates with sizes of 1 to 3 μm in the spaces between as-solidified dendrites (Fig. 18f). Combining with the result obtained from X-ray diffraction, the phase may be considered as Al_7Cu_4Li.

5. Conclusions

1. The method of explosive consolidation is suitable for obtaining Al and Al–Li alloy compacts with a relative density of more than 98% and rather large dimensions, as long as the explosive parameters, capsule design and other operations fulfil certain requirements.

2. The as-solidified dendritic microstructures in atomized powders are preserved during explosive consolidation. The optically featureless region which appears in explosive Al–Li alloy compact is a recrystallized zone consisting of ultrafine grains; it is evidently the result of the melting and resolidifying of

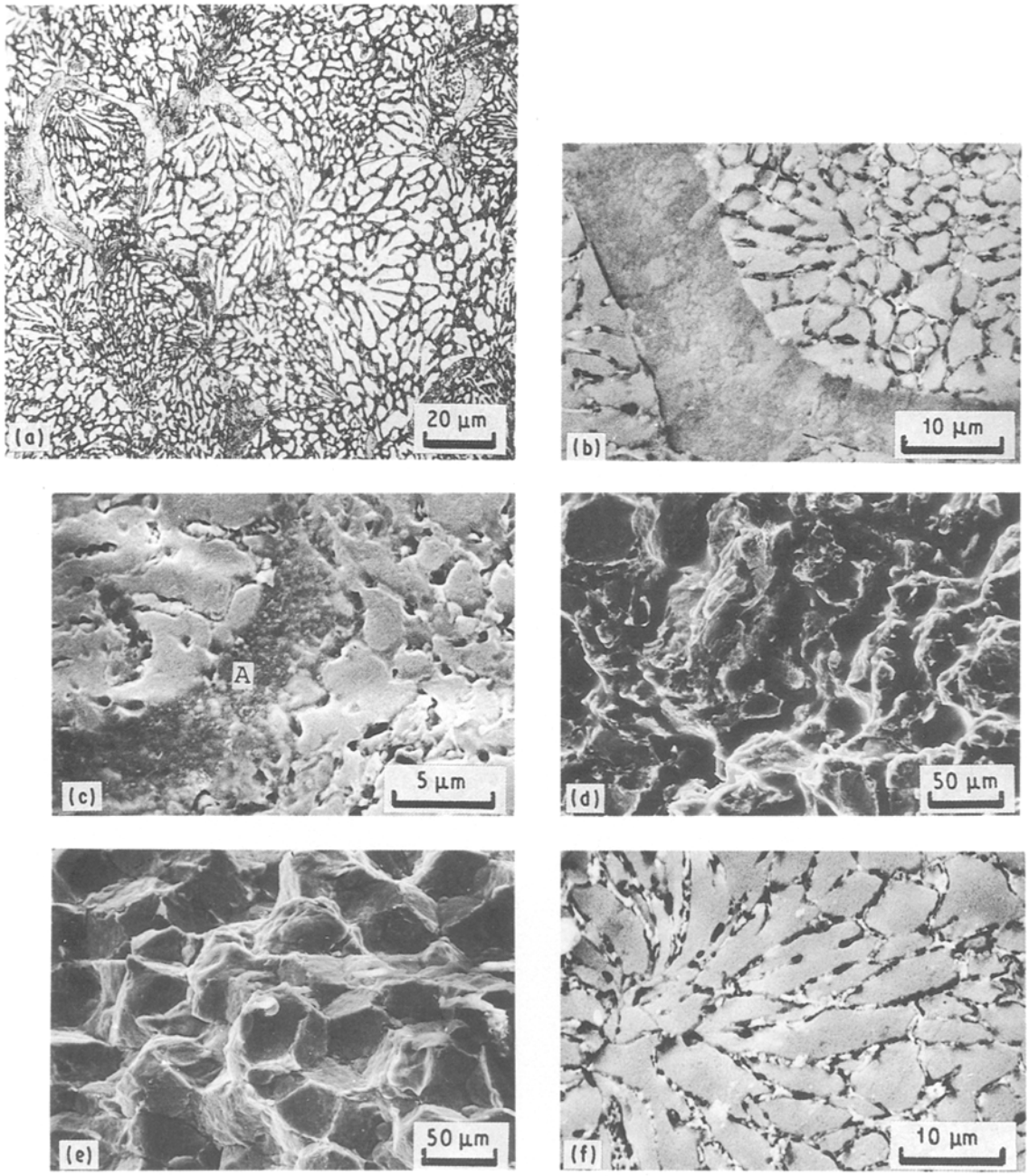

Figure 18 Micrographs and fractographs of explosively consolidated ultrasonic argon-atomized Al–Li alloy powder: (a) optical micrograph of polished and etched specimen showing optically featureless region, (b) scanning electron micrograph of polished and etched specimen, (c) scanning electron micrograph of the specimen at higher magnification showing an ultrafine recrystallized zone, (d) scanning electron fractograph of the compact, (e) scanning electron fractograph of the compact, (f) scanning electron micrograph showing precipitates.

particle surfaces at much a higher cooling rate during explosive consolidation.

3. The characteristics of the oxide layers on the surfaces of powder particles play a key role in determining the effectiveness of the joints between powder particles; the oxide layers must be broken up during explosive consolidation in order to obtain an acceptable mechanical property of the compact.

4. The explosive Al–Li alloy compacts present an abnormal softening appearance compared to the original powder.

Acknowledgements

The General Research Institute for Non-Ferrous Metals, Beijing, is acknowledged for supplying the Al–Li alloy powder and the laboratories for Explosive Experiments of the Institute of Mechanics Research, Academina Sinica, for providing the conditions suitable for explosive experiments. The authors also wish to thank Sheng Chen and Yubao Li for their assistance in the experiments.

References

1. T. J. CARNEY, *Metal Powder Rep.* **43** (1988) 266.
2. "Dynamic Compaction of Metal and Ceramic Powders", NMAB-394, National Materials Advisory Board, National Academy of Sciences, USA, 1983.
3. R. PRUMMER, in "Explosive Welding, Forming, and Compaction", edited by T. Z. Blazyuski (Applied Science, London, 1983) p. 369.
4. D. G. MORRIS, *Mater. Sci. Engng.* **57** (1983) 187.

5. T. C. PENG, S. M. L. SASTRY and J. E. ONEAL, *Met. Trans.* **16A** (1985) 1445.
6. JIN-YUAN ZHANG and S. J. SAVAGE, *Scand. J. Metall.* **17** (1988) 182.
7. H. JONE, "Rapid Solidification of Metals and Alloys" (Institution of Metallurgists, London, 1982) p. 42.
8. P. S. GILMAN and K. K. SANKARAN, Metal Powder Report 43 (1988) 428.
9. T. C. PENG, S. M. L. SASTRY and R. J. LEDERICH, in Mechanical Behaviour of Rapidly Solidified Materials, M. L. Shanker, edited by (Metallurgical Society, Inc., Warrendale, Pa. 1986) p. 181.

Received 20 February
and accepted 3 December 1990